APEM journal
**Advances in Production Engineering & Management** **ISSN 1854-6250**
Volume 9 | Number 2 | June 2014 | pp 71–82 Journal home: apem-journal.org
http://dx.doi.org/10.14743/apem2014.2.177 Original scientific paper

# Determining the optimal area-dependent blank holder forces in deep drawing using the response surface method

**Volk, M.**[a,*], **Nardin, B.**[a], **Dolsak, B.**[b]

[a]Gorenje Orodjarna, d.o.o., Velenje, Slovenia
[b]University of Maribor, Faculty of Mechanical Engineering, Maribor, Slovenia

**A B S T R A C T**

Metal forming processes are often currently highly automated mass production processes for manufacturing a wide variety of metal parts from various industries. Maximizing product quality and consequently minimizing waste and production costs are major goals for those companies exploiting metal forming processes. On the other hand, sheet metal parts become more complex especially because of complex product designs and the usages of higher strength steels that have less formability. Therefore, metal forming processes need to be optimized. This research study demonstrates an optimization system for optimizing the sheet metal forming process using the Finite Element Method (FEM) combined with the Response Surface Method (RSM). The proposed optimization system was tested on an industrial example from the household appliances industry. In this study, it is described as to how to determine optimal area-dependent blank-holder forces in deep drawing process in order to obtain the best possible quality of the drawing part. The optimization system consists of three main steps: modeling, screening, and optimization. The results showed that with better preferences regarding the blank-holder forces, better results can be achieved. Forming and spring-back criteria were taken into account. The number of required numerical simulations using the RSM combined with the Design of Experiment was not critical and was much smaller than using other conventional optimization methods. Therefore, reasonably accurate results can be achieved in a relativity short time, which is one of the main advantages of this method.



**A R T I C L E  I N F O**

*Keywords:*
Sheet metal forming
Optimization
Finite element method
Response surface method

**Corresponding author:*
mihael.volk@gorenje-orodjarna.si
(Volk, M.)

*Article history:*
Received 6 December 2013
Revised 30 May 2014
Accepted 3 June 2014

## 1. Introduction

Despite all of the new technologies and improvements in sheet metal forming processes, the forming tools for deep drawing have not significantly changed. The production tools and deep drawing processes are very rigid, therefore it is very hard to improve the quality of the products without extra expenses. On the other hand, deep drawn products become more complex, thus creating additional problems for the toolmakers. Basically, the only (and the most influenced) parameter which can be optimized without encroaching into the tool, and which can be controlled, is a blank holder force (BHF) [1].

Many researchers used BHF for improving the quality of the drawing parts [1-16] and most of them described BHF with the technological window (Fig. 1). An excessive value of BHF causes fracture, whilst an insufficient value of BHF will result in wrinkles [4, 5].

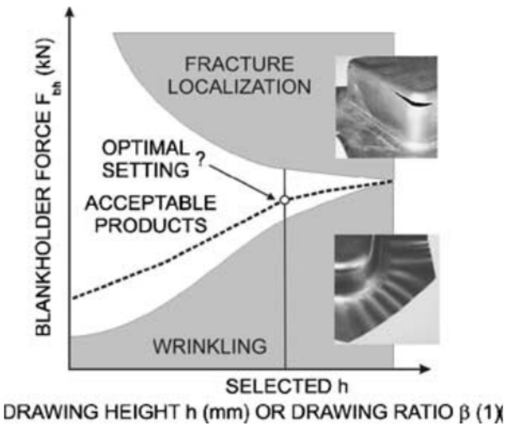


**Fig. 1** Technological window [4]

Beside wrinkles and fractures, one of the most important problems is spring-back [10, 12] and the BHF has a large influence on it [9, 13]. Spring-back in sheet-metal forming can be described as the change in the sheet-metal's shape compared with the shapes of the tools after the forming process [8]. We differentiate the following types of spring-back when considering the geometry of a product: angular change, sidewall curl, and twist (Fig. 2).

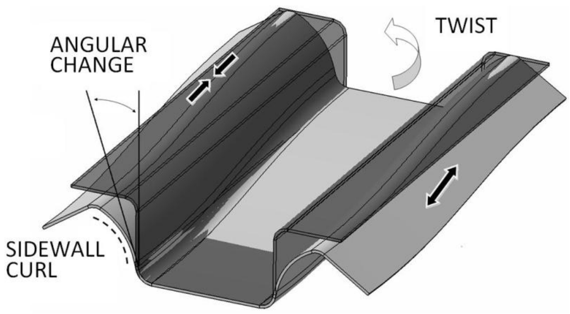


**Fig. 2** Types of spring-back [10]

Because BHF seems to be one of the most important parameters in sheet metal forming, a new holding system with segment inserts was developed. This holding system is described in [9, 13] and belongs to holding systems which can provide variable BHFs to the sheet metal [5-8]. While using this holding system, the stamping process is more controlled, the processing window is wider, and the process is more stable [9]. However, finding the optimal configuration of blank holder forces is critical and requires several experimental tests when using conventional optimization methods [5, 9, 15, 16].

This research study presents a method for finding the optimal configuration of blank holder forces. The mathematical approximation algorithm called the response surface method (RSM) and results of finite element numerical simulations were used. Design Expert 8.0 and Pam-stamp 2011 software packages were also used in this research study. The presented method was tested on the deep drawing process but could be used for other applications as well.

## 2. Used methods

In this research study, the response surface method (RSM) with the combination of finite element method results was used. The response surface methodology is a collection of mathematical and statistical techniques useful for the modeling and analysis of problems in which a response of interest is influenced by several variables, and the objective is to optimize this response [17].

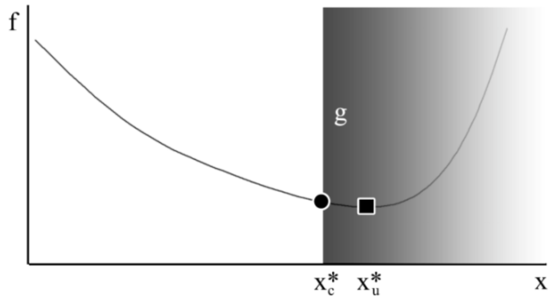


**Fig. 3** Mathematical optimization [17]

In general, the optimization method could be described as a mathematical problem in which we are seeking to minimize or to maximize a certain function by systematically choosing the values of certain variables which are allowed to be adopted [18]. Figure 3 presents a function $f$ that needs to be minimized by adopting the variable $x$. The results of mathematical optimization is the optimum $x_u$* where function $f$ reaches minimum value. However, in many practical problems, certain restrictions $g$ or unwanted areas (the shaded area in the Fig. 3) are present. If we also take into consideration those restrictions, then the optimum of the mathematical optimization is not at $x_u$* anymore, but at $x_c$*.

The success of the prediction and optimization critically depends on the ability to develop a suitable approximation for the actual response $f$ of the system. With the RSM the response $f$ is predicted by polynomial models.

A first order polynomial model is given by Eq. 1 [16]

$$y = \beta_0 + \sum_{i=1}^{k} \beta_i x_i + \varepsilon \tag{1}$$

A second order polynomial model also called as quadratic model is given by Eq. 2 [17]

$$y = \beta_0 + \sum_{i=1}^{k} \beta_i x_i + \sum_{i=1}^{k} \beta_{ii} x_i^2 + \sum\sum_{i<j} \beta_{ij} x_i x_j + \epsilon \tag{2}$$

where $k$ is the number of design variables, $x_i$ is the set of design variables, $\beta$ are polynomial coefficients and ∈ is minor error.

For many RSM problems, either first or second order models are used. Higher ordered models are not desired due the high amount of experimental data needed for the prediction of the response $f$.

Nowadays, RSM is used in many applications for solving complex problems which normally requires substantial testing data. In the past, it was also used in some experimental cases of optimizing sheet metal forming processes [19-21].

## 3. Description of the proposed system

The proposed optimization system consists of 3 main steps: modeling, screening, and optimization (Fig. 4).

The optimization system was developed for deep drawing optimization problems but could also be used for other problems. Some steps can differ or can be skipped in these cases. In the following sections, the optimization system is going to be shown, especially for deep drawing processes.

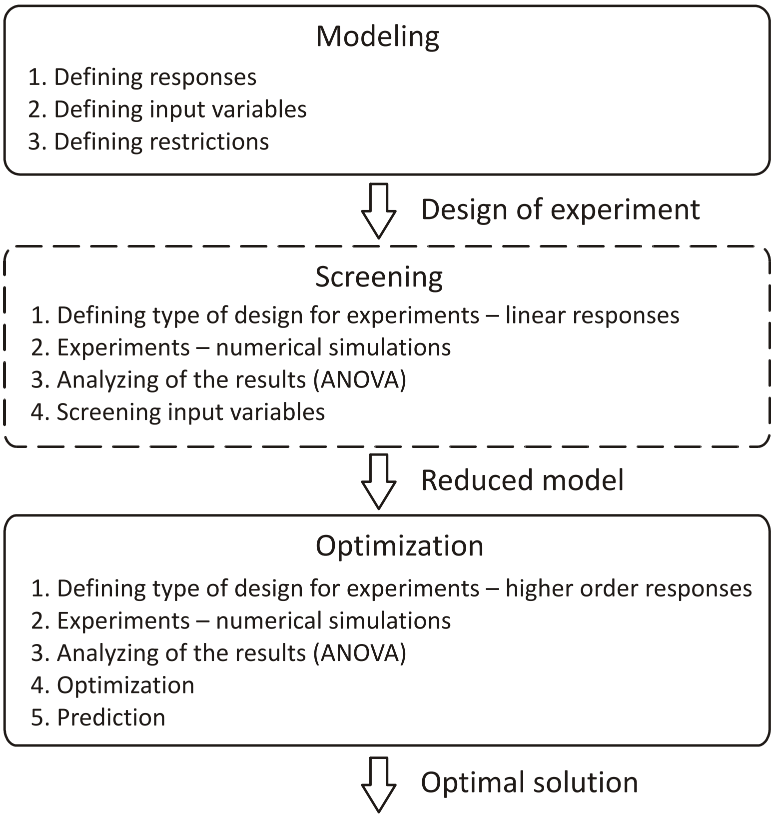


**Fig. 4** Proposed optimization system

### 3.1 Modeling

Modeling is the first step of this optimization procedure. In the modeling step responses, the input variables and restrictions have to be defined. This step depends mostly on the optimization problem which we are going to solve.

*Defining responses*

In practice, it is common that problems have more than one response. In this research study, we defined responses based on faults which can happen during the deep drawing processes. Many of those faults can be described as forming faults (FF) and faults due to spring-back (FSB), Table 1. Among FF we can include cracks, wrinkles, insufficient stretching and excessive thinning, and into FSB we can count deviations of shape, angular change and twist (Fig. 1 and Fig. 2).

Most of the FF can be well defined based on the forming limit diagram (Fig. 5). The finite element (FE) nodes which lay in area V and VI mean that the product will wrinkle; those which lay in area III will crack and those in IV are safe. Areas I and II are also not desirable because of biaxial tension deformation which can lead to excessive thinning. Therefore, a thinning parameter can be used for avoiding areas I, II, and III.

**Table 1** Responses

| | Fault | Goal | Fault | Goal | Fault | Goal | Fault | Goal |
|---|---|---|---|---|---|---|---|---|
| FF | Wrinkling trend (%) | 0 % | Crack (%) | 0 % | Insufficient stretching (%) | 0 % | Thinning (mm) | Minimum |
| FSB | Angular change $\alpha$ (°) | 0° | Angular change $\beta$ (°) | 0° | Twist (°) | 0° | Maximum deviation (mm) | Minimum |

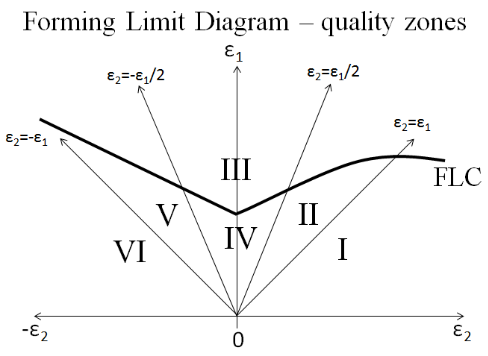


**Fig. 5** Forming limit diagram

Among the FSB we can count angular change, twist, and deviations from the reference shape of the drawing part. For this particular part, the angular change was measured in 3 sections (Fig. 6). The sections are equally divided; section 1 is on the symmetry plane, section 2 is 150 mm from the symmetry plane and section 3 is 300 mm from the symmetry plane. The twist was calculated as the angle between plane normal at section 1 and section 3. On the other hand, deviations are represented as the deviation between nodes before and after spring-back. Maximum deviations were taken into consideration.

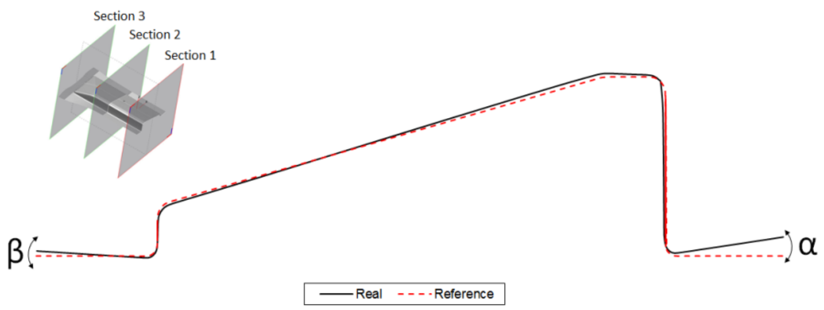


**Fig. 6** Spring-back – angular change α and β

*Defining input variables*

In this research study, the main goal is to optimize the area-dependent BHFs to maximize the part quality of the deep drawing part (Fig. 7). Taking into account the symmetry, the BHF is divided into 6 different areas BHF1, BHF2, BHF3, BHF8, BHF9, and BHF10 which were selected as input variables. In total, this optimization problem therefore consists of 6 different input variables.

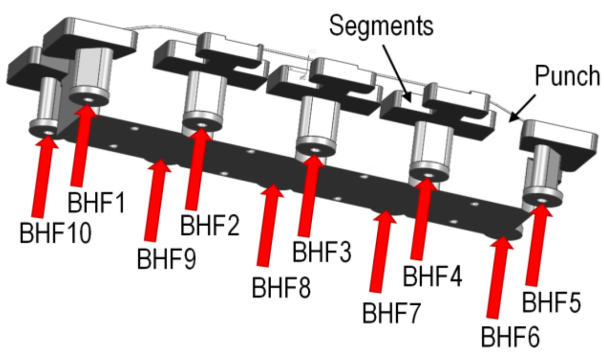


**Fig. 7** Input variables – blank holder forces

*Defining restrictions*

The range of BHFs was determined based on press capability and previous experience. Minimal BHF for each segment was 20 kN and maximal BHF was 60 kN. All ranges and levels of input variables in this study are presented in Table 2.

**Table 2** Input variables and their ranges and levels

| Factor | Variable | Unit | Min | Mean | Max |
|---|---|---|---|---|---|
| A | BHF1 | kN | 20 | 40 | 60 |
| B | BHF2 | kN | 20 | 40 | 60 |
| C | BHF3 | kN | 20 | 40 | 60 |
| D | BHF8 | kN | 20 | 40 | 60 |
| E | BHF9 | kN | 20 | 40 | 60 |
| F | BHF10 | kN | 20 | 40 | 60 |

### 3.2 Screening

In this research study, the main goal was to optimize the BHFs. Including the symmetry plane, we had to optimize 6 different BHFs. The main purpose of the screening stage is to minimize the number of input variables. However, there is no need for that in this case because the system is already reduced to only 6 input variables; the number of experimental data is not significantly large and time for numerical simulations is not critical. Therefore, the screening stage was skipped. As this stage was not necessary, it is also marked differently on Fig. 4. This stage seems to be increasingly useful when the complexity of the system grows. The reasonable limit for the RSM is around 8 input variables. If the system consists of more than 8 input variables, then it is advisable to use a screening stage.

The screening stage procedure is very similar to the optimization step with the difference that the screening stage results are analysed on simple linear responses. However, for the optimization higher order polynomials are usually needed. With this simplification, the experimental plans have less data and therefore more input variables can be analysed in a relatively short time, even if the results are not always accurate. However, they are still adequate enough that the trend and the influence of the input variable can be noticed.

### 3.3 Optimization

Optimization was done based on RSM. Firstly, the experimental plan was made. It was made based on the central composite design (CCD) which gives a good approximation for the second order polynomial. The experimental plan made with CCD consists of $N = 2^k + 2k + N_c$ experiments, where $k$ is the number of input variables and $N_C$ is number of central points. In case in which the results of numerical simulations are used, the central points don't have to be multiplied, therefore the total number of central point is 1. The reason for this is that numerical simulations with the same input parameters will always give the same result. The whole experimental plan can be found in [22] and count to a total of 77 experiments for 6 input variables.

The next step is to analyse the results based on Analysis of Variance (ANOVA) [23]. This step is covered in section 5.1.

The last step of the optimization is to find the optimum input variables in order to increase the quality of the deep drawing part. This can be done using criteria function $D$ (Eq. 3)

$$D = (D_1^{r1} \times D_2^{r2} \times \ldots \times D_n^{ri})^{\frac{1}{\sum ri}} \tag{3}$$

where $D_n$ is a criterion function for each response, and $r_i$ is the importance of the response. With this optimization method we get a list of solutions, and the solution with the highest number is the best solution. The value of $D$ can be in the range from 0 to 1. Results with $D = 1$ are the solutions which satisfy our goals.

## 4. Method verification on industry case

The presented method for optimization has been verified on an industry case from the household appliances industry. The main goal in this case was to optimize the quality of the front panel product (Fig. 8). For this purpose, a testing die was made with blank holder with 10 segments inserts (Fig. 7 and Fig. 9). The part is symmetrical in one plane and therefore only half of the part was taken for the investigation.

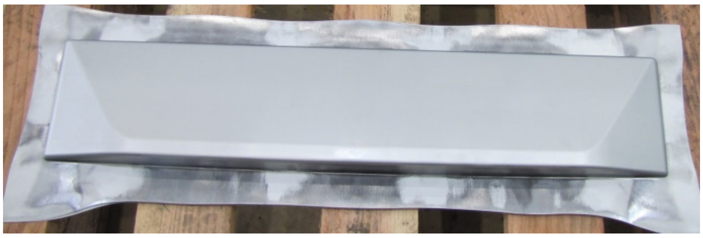

**Fig. 8** Front panel

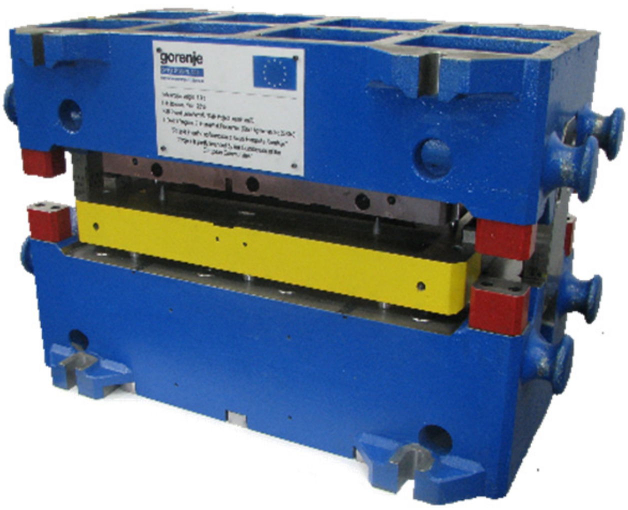

**Fig. 9** Testing die

*Material properties*

A commercially-available DC04 sheet metal with a nominal thickness of 0.7 mm was used for the sheet material.

The material characteristics of the sheet metal have been conducted by uniaxial tensile tests. Tensile tests have been carried out on a Zwick/Roell 1474 machine based on SIST standards. The specimens have been cut at angles 0°, 45°, and 90° with respect to the rolling direction and for each direction five tensile tests have been performed. For the numerical calculations, Hill48 with orthotropic anisotropy was used. The material model's coefficients were identified based on stress-strain curves (Table 3).

**Table 3** Material properties of sheet metal

| | | |
|---|---|---|
| Blank material | DC04 | |
| Nominal thickness | 0.7 mm | |
| Yield strength | 188.9 N/mm$^2$ | |
| Tensile strength | 298.4 N/mm$^2$ | |
| Strength coefficient | 558.8 N/mm$^2$ | |
| Hardening exponent | 0.22 | |
| | 0° | 1.67 |
| Coefficient of anisotropy | 45° | 1.45 |
| | 90° | 1.818 |

The strain-stress hardening curve has been defined by tensile test and extrapolated with Hollomon's hardening law given by Eq. 4 (Fig. 10)

$$\sigma_f = C \times \varepsilon^n \tag{4}$$

where $\sigma_f$ is yield stress, $C$ is strength coefficient, ε is true strain, and $n$ is hardening exponent.

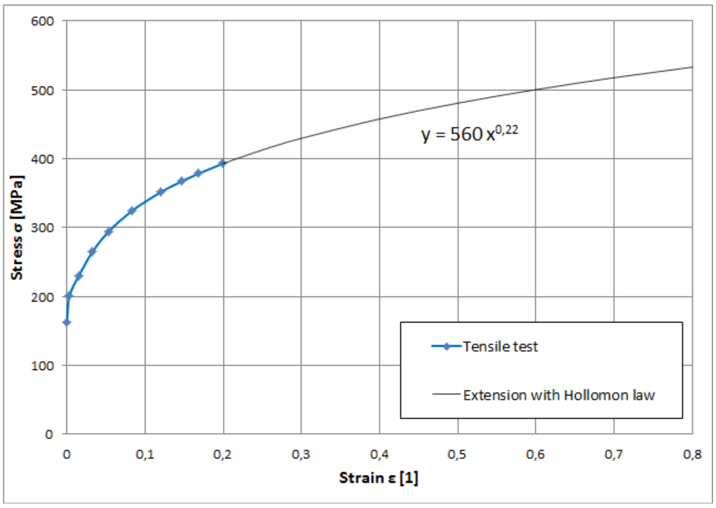


**Fig. 10** Strain-stress curve

The forming limit curve (FLC) in Fig. 11 was calculated by the predictive method [24]. The main advantage of this method is that it accurately predicts FLC with the help of mechanical properties A80 which are obtained with the uniaxial tensile test, the *r*-values and the sheet thickness. No other data is needed.

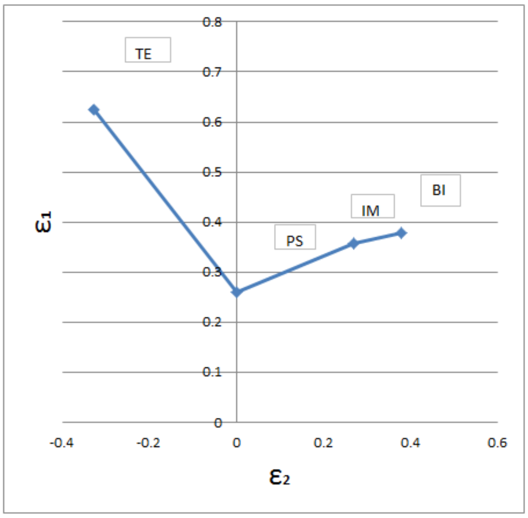


**Fig. 11** Forming limit diagram

## 5. Results and discussion

The results were evaluated to suit the requirements of the selected design of experiments. All the numerical results were analysed through RSM. For this purpose, the quadratic models were mainly used to explain the mathematical relationship between input variables and objective functions. Quadratic polynomial equation for one objective function "thinning" was:

$$Thinning = E^{-5} \times (18459 + 16.8A - 68.5B - 450C - 27.9D + 135.5E + 316.8F - 2.48AD + 2.48AF - 2.96BC + 1.94CD + 2.99CE - 2.9CF + 1.5DE - 3.92DF + 1.9B^2 + 6.26C^2 + 4.04D^2 - 1.89E^2) \quad (5)$$

## 5.1 ANOVA

The results of ANOVA presented in this section are presented for only one objective function "thinning". The results for this objective function are shown in Table 4 and indicate that the predictability of the model for thinning is in 99% confidential interval. The predicted responses fit well with those of the numerically obtained results. The coefficients of determination ($R^2$) values close to 1 indicate that polynomial approximation (Eq. 5) is highly reliable. *F*-value is greater than that of the tabular $F_{0.01}$ [15] and *p*-value is low which suggest that the model influence on the objective function is statistically significant.

**Table 4** ANOVA result for the "thinning" objective function in reduced quadratic model

| | Sum of squares | Number of factors | Standard deviation | *F*-value | *p*-value |
|---|---|---|---|---|---|
| Model | 0.032921 | 18 | 0.001829 | 21.6705 | < 0.0001 |
| A-BHF1 | 8.37E-06 | 1 | 8.37E-06 | 0.099115 | 0.7540 |
| B-BHF2 | 0.000754 | 1 | 0.000754 | 8.939431 | 0.0041 |
| C-BHF3 | 0.006624 | 1 | 0.006624 | 78.48896 | < 0.0001 |
| D-BHF8 | 0.008627 | 1 | 0.008627 | 102.221 | < 0.0001 |
| E-BHF9 | 0.000914 | 1 | 0.000914 | 10.83443 | 0.0017 |
| F-BHF10 | 0.005354 | 1 | 0.005354 | 63.44184 | < 0.0001 |
| AD | 0.000327 | 1 | 0.000327 | 3.875955 | 0.0538 |
| AF | 0.000159 | 1 | 0.000159 | 1.879241 | 0.1757 |
| BC | 0.000964 | 1 | 0.000964 | 11.4271 | 0.0013 |
| CD | 0.00034 | 1 | 0.00034 | 4.029295 | 0.0494 |
| CE | 0.000917 | 1 | 0.000917 | 10.86932 | 0.0017 |
| CF | 0.000436 | 1 | 0.000436 | 5.171731 | 0.0267 |
| DE | 0.000229 | 1 | 0.000229 | 2.709674 | 0.1052 |
| DF | 0.000785 | 1 | 0.000785 | 9.305206 | 0.0034 |
| B^2 | 0.000254 | 1 | 0.000254 | 3.004378 | 0.0884 |
| C^2 | 0.002791 | 1 | 0.002791 | 33.07372 | < 0.0001 |
| D^2 | 0.001108 | 1 | 0.001108 | 13.12282 | 0.0006 |
| E^2 | 0.000225 | 1 | 0.000225 | 2.66841 | 0.1078 |
| $R^2$=0.870555665; Adj. $R^2$=0.830383285; pred. $R^2$=0.776865668 | | | | | |

## 5.2 Optimization

Optimization is made based on the results which are predicted by the polynomial. The optimization system predicts a set of solutions with different BHFs and belonging values of objective functions. All results can be presented graphically with the response surface (Fig. 12). This Figure presents results based on BHF4, BH6 and desirability which is a parameter describing the achievement of our goals. It is calculated by Eq. 2. The solution on the top of the surface presents the best solution with a highest value of D. All input parameters for these solutions are shown in Table 5.

**Table 5** Best solution chosen based on desirability

| Variable | BHF1 | BHF2 | BHF3 | BHF8 | BHF9 | BHF10 |
|---|---|---|---|---|---|---|
| Value (kN) | 43 | 54 | 35 | 48 | 60 | 30 |

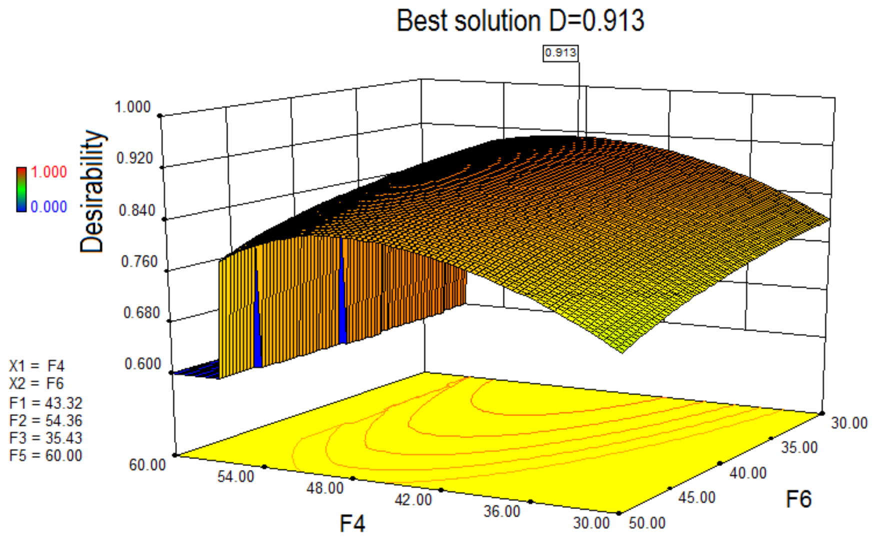


**Fig. 12** Response surface of all solutions

## 5.3 Comparing with FEM results

At the end of this research study, we checked if the optimal solution is really better than the previous one. We checked this by comparing numerical results made with BHFs before and after this optimization. This comparison is described in Fig. 13 and in Table 6. The results showed a significant improvement of all quality parameters. This has proven the usefulness of the presented method, and its great potential for the optimization of sheet metal forming processes.

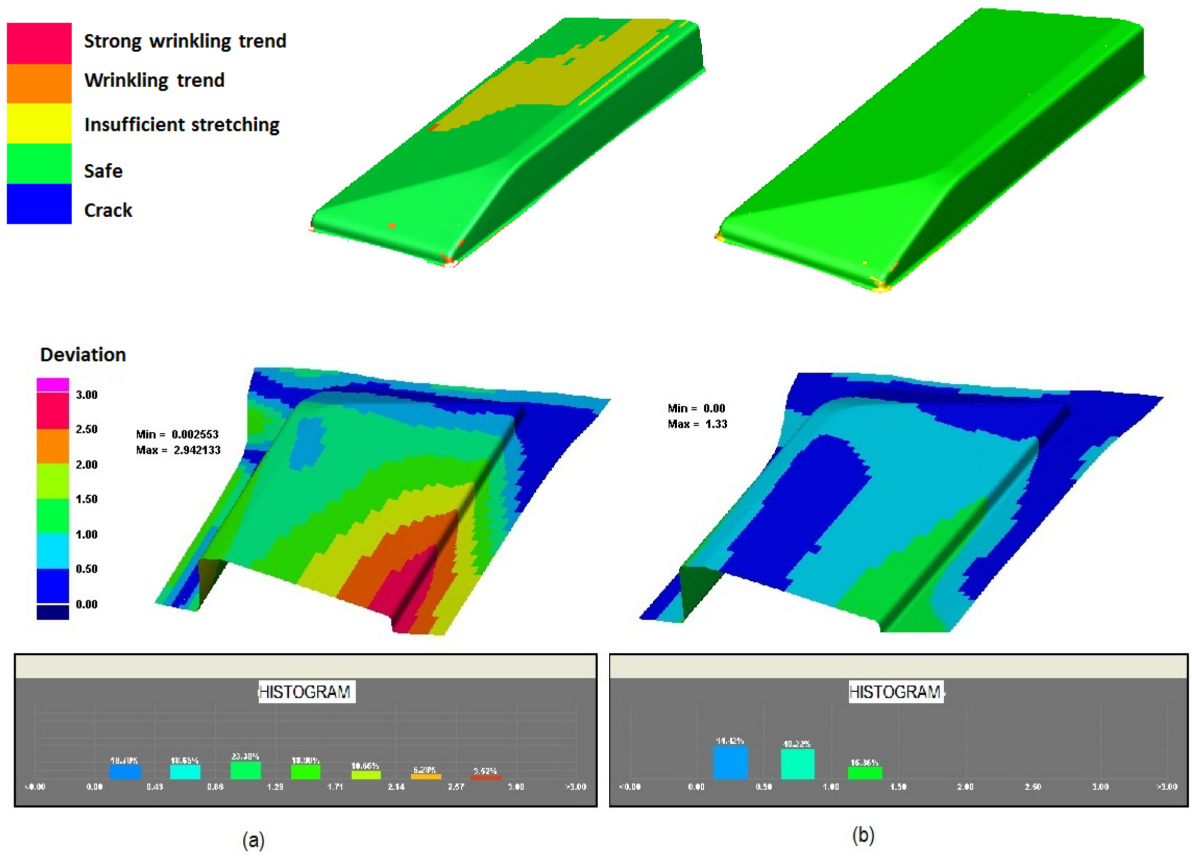


**Fig. 13** Comparison of the results before and after optimisation

**Table 6** Comparing numerical results before and after optimisation

| Objective function | Wrinkling trend | Crack | Insufficient stretching | Thinning | Maximum deviation |
|---|---|---|---|---|---|
| Before optimization | 2.27 % | 0.02 % | 24.08 % | 21.5 % | 2.94 |
| After optimization | 0.42 % | 0 % | 0 % | 20.9 % | 1.33 |
| Improvements | +82 % | - | +100 % | +3 % | +55 % |

Fig 13. graphically shows improvement in the part quality. The upper two figures show that more area which represents safe area (FE nodes which lay in area IV on Fig 5.) is present on the right part. The lower two figures show deviations between FE nodes before and after spring-back. The right optimized part has fewer deviations.

Even better improvements can be seen in Table 6. The improvements shown are significant. For the quality parameter "crack" the improvements in % is not calculated because the defect after optimization is 0 % and even before optimization the % was very low.

Reported results show that by using this optimization system, reasonably good results and improvements can be achieved in a relatively short time. This optimization can be done during the development of the manufacturing method for the part, which could be a substantial benefit later in the production. The accuracy of the results strongly depends on the accuracy of the numerical models. However, numerical simulations are becoming increasingly reliable; therefore, this optimization system will become even more valuable.

## 6. Conclusion

This research study presents the newly developed optimization system for optimising deep drawing parameters in order to get better part quality. The optimization system consists of three steps: modeling, screening and optimization. The methodology incorporates RSM and the results of FEM; the optimum area-dependent BHFs are determined with FEM and RSM by optimizing the objective function related with variables that are very difficult to determine during try-outs, as well as very time consuming.

At the end of this research study, the optimization system was tested on the industrial example from the household appliances industry. It took into account the most important input variables and unwanted output properties (as objective functions) of the part. Results showed that with optimization of the process and area-dependent BHF, that it is possible to achieve the better part quality. The optimization system was developed for deep drawing optimization problems, but could also be used for other problems in various fields.

## Acknowledgement

Operation part financed by the European Union, European Social Fund.

## References


[1] Tisza, M. (2013). Recent development trends in sheet metal forming, *International Journal of Microstructure and Materials Properties,* Vol. 8, No. 1/2, doi: 10.1504/IJMMP.2013.052651.

[2] Albut, A., Ciubotaru, V., Radu, C., Olaru, I. (2011). Optimization of the blank holder force using neural network algorithm, In: *AIP Conf. Proc. 1383*, Vol. 1383, 1004-1009, doi: 10.1063/1.3623714.

[3] Liewald, M., Wurster, K., Blaich, C. (2011). New approaches on automated wrinkle detection in sheet metal components by forming simulation, In: *AIP Conf. Proc. 1353,* 1185-1190, doi: 10.1063/1.3589677.

[4] Gantar, G., Kuzman, K., Filipič, B. (2005). Increasing the stability of the deep drawing process by simulation-based optimization, *Journal of Materials Processing Technology,* Vol. 164-165, 1343-1350, doi: 10.1016/j.jmatprotec.2005.02.099.

[5] Kitayama, S., Hamano, S., Yamazaki, K., Kubo, T., Nishikawa, H., Kinoshita, H. (2010). A closed-loop type algorithm for determination of variable blank holder force trajectory and its application to square cup deep drawing, *The International Journal of Advanced Manufacturing Technology,* Vol. 51, No. 5-8, 507-517, doi: 10.1007/s00170-010-2656-9.

[6] Palaniswamy, H., Braedel, M., Thandapani, A., Altan, T. (2006). Optimal programming of multi-point cushion systems for sheet metal forming, *CIRP Annals – Manufacturing Technology,* Vol. 55, No. 1, 249–254, doi: 10.1016/S0007-8506(07)60409-0.

[7] Neugebauer, R., Leib, U., Bräunlich, H., (1997). Influence on materials flow in deep drawing using individual controllable draw pins and smooth blankholder design, In: *Proceedings of SAE International Congress & Exposition*, Detroit, Michigan, SEA Paper No. 970989, 269-274, doi: 10.4271/970989.

[8] Endelt, B., Tommerup, S., Danckert, J. (2009). A novel feedback control system – Controlling the material flow in deep drawing using distributed blank-holder force, *Journal of Materials Processing Technology,* Vol. 213, No. 1, 36–50, doi: 10.1016/j.jmatprotec.2012.08.003.

[9] Volk, M., Deželak, M., Nardin, B., Stepišnik, S. (2012). Prediction of the spring-back calculated with numerical simulations for the household industry, In: *AIP Conf. Proc. 1383*, 1078-1085, doi: 10.1063/1.3623723.

[10] Deželak, M., Pahole, I., Stepišnik, A., Fijavž, R. (2011). Finite element method combined with machine learning for springback prediction, In: *6th International Conference and Exhibition on Design and Production of Machines and Dies/Molds,* Atilim University, Ankara, Turkey, 83-87.

[11] Dezelak, M., Stepisnik, A., Pahole, I., Ficko, M. (2014). Evaluation of twist springback prediction after an AHSS forming process, *International Journal of Simulation Modelling*, Vol. 13, No. 2, 171-182, doi: 10.2507/IJSIMM13(2)4.261.

[12] Tang, L., Wang, H., Li, G. (2013). Advanced high strength steel springback optimization by projection-based heuristic global search algorithm, *Materials & Design,* Vol. 43, 426-437, doi: 10.1016/j.matdes.2012.06.045.

[13] Volk, M., Nardin, B., Dolšak, B. (2011). Application of numerical simulations in the deep-drawing process and the holding system with segments' inserts, *Strojniški vestnik – Journal of Mechanical Engineering,* Vol. 57, 697-703, doi: 10.5545/sv-jme.2010.258.

[14] Albut, A., Ciubotaru, V., Radu, C., Olaru, I. (2011). Optimization of the blank holder force using the neural network algorithm, In: *AIP Conf. Proc.* 1383, 1004-1009, doi: 10.1063/1.3623714.

[15] Intarakumthornchai, T., Jirathearanat, S., Juntaratin, J. (2011). Determination of loading paths in hydromechanical deep drawing process of parabolic cup with FEA based 2-D interval halving and fuzzy logic, In: *Proceedings of the 4th International Conference on Modelling and Simulation of Metallurgical Processes in Steelmaking – Metec Insteelcon 2011,* Düseldorf, Germany.

[16] Kitayama, S., Kita, K., Yamazaki, K. (2012). Optimization of variable blank holder force trajectory by sequential approximate optimization with RBF network, *The International Journal of Advanced Manufacturing Technology,* Vol. 61, No. 9-12, 1067-1083, doi: 10.1007/s00170-011-3755-y.

[17] Montgomery, D.C. (2012). *Design and analysis of experiments*, 5th ed*., Wiley,* New York.

[18] Bonte, M.H.A. (2007). Optimisation strategies for metal forming processes, PhD Thesis, University of Twente, Enschede, The Netherlands.

[19] Intarakumthornchai, T., Jirathearanat, S., Thongprasert, S., Dechaumphai, P. (2010). FEA based optimization of blank holder force and pressure for hydromechanical deep drawing of parabolic cup using 2-D interval halving and RSM methods, *Engineering Journal,* Vol. 14, No. 2, 15-32, doi: 10.4186/ej.2010.14.2.15.

[20] Velmanirajan, K., Thaheer, A.S.A., Narayanasamy, R., Ahamed Basha, C. (2012). Numerical modelling of aluminium sheets formability using response surface methodology, *Materials & Design,* Vol. 41, 239-254, doi: 10.1016/j.matdes.2012.05.027.

[21] Sun, G., Li, G., Gong, Z., Cui, X., Yang, X., Li, Q. (2010). Multiobjective robust optimization method for drawbead design in sheet metal forming, *Materials & Design,* Vol. 31, No. 4, 1917-1929, doi: 10.1016/j.matdes.2009.10.050.

[22] Volk, M. (2013). Stabilization of the deep drawing process with sheet metal holding control, PhD Thesis, (original title: Stabilizacija procesa globokega vleka z obvladovanjem pridrževanja pločevine), University of Maribor, Faculty of mechanical engineering, Maribor, Slovenia.

[23] Hribernik, A. (2011). Methods of experimental work: design of experiments (original title: Metode eksperimentalnega dela: načrtovanje eksperimentov), University of Maribor, Faculty of mechanical engineering, Maribor, Slovenia.

[24] Abspoel, M., Scholting, M.E., Droog, J.M.M. (2012). A new method for predicting forming limit curves from mechanical properties, *Journal of Materials Processing Technology*, Vol. 213, No. 5, 759-769, doi: 10.1016/j.jmatprotec.2012.11.022.